J. Electrochem. Sci. Eng. **16** (2026) 3189; https://doi.org/10.5599/jese.3189

Open Access : : ISSN 1847-9286
https://pub.iapchem.org/ojs/index.php/JESE

Original scientific paper

Synergistic effects of NH_2-MIL-101(Fe) metal-organic framework and Pd nanoparticles for sensitive determination of norepinephrine in the presence of acetaminophen

Shaimaa A. Jadoo, Azhar Farooq, Israa M Radhi, Hanadi A. Fadhil and Juman A. Naser✉

University of Baghdad, College of Education for Pure Science- Ibn Alhaitham, Department of Chemistry, Baghdad, Iraq

Corresponding Author: ✉juman.a.n@ihcoedu.uobaghdad.edu.iq

Received: December 28, 2025; Revised: March 22, 2026; Published: April 3, 2026

Abstract

An electrochemical sensor based on an amino-functionalized iron NH_2-MIL-101(Fe) metal-organic framework (MOF)/Pd nanoparticles (NPs) composite-modified screen-printed electrode (SPE) is prepared for the simultaneous determination of norepinephrine (NEPI) and acetaminophen (ACP). The NH_2-MIL-101(Fe) MOF/Pd NPs/SPE electrochemical sensor shows a significant enhancement in the response peak current of NEPI, as compared to bare SPE. This suggests that the unique features of NH_2-MIL-101(Fe) MOF/Pd NPs composite-modified SPE improve the electrocatalytic oxidation of NEPI. Such a synergistic effect between NH_2-MIL--101(Fe) MOF and Pd NPs results in a significant enhancement in the response, where the MOF's high surface area combines with the high electron-transfer rate and the abundance of catalytically active sites afforded by the Pd NPs. The differential pulse voltammetry (DPV) method was obtained for quantitative determination of NEPI and high sensitivity was observed in NEPI determination with the calibration slope of 0.0327, μA $μM^{-1}$. The developed NH_2-MIL-101(Fe) MOF/Pd NPs/SPE sensor presents a low limit of detection of 0.007 μM toward NEPI determination. The developed NH_2-MIL-101(Fe) MOF/Pd NPs/SPE sensor shows a good catalytic activity for the oxidation of NEPI and ACP, with anodic peak potentials of 360 and 550 mV, respectively. The separation of anodic peak potential is sufficient to enable simultaneous determination. Finally, the suggested sensing platform has confirmed suitable for the simultaneous determination of NEPI and ACP in real samples (pharmaceutical formulations and urine samples), achieving recovery values ranging from 97.1 to 104.4 % with relative standard deviations ≤3.6 %.

Keywords

Electrochemical sensor; screen-printed electrode; nanoparticles; norepinephrine; acetaminophen.

Introduction

Noradrenaline (NEPI), also called norepinephrine, is a neurotransmitter in the mammalian central nervous system [1]. It is an important neurotransmitter in the nervous system. Already, it is known that NEPI plays a role in the regulation of emotions, attention, mood, learning and stress response [2,3]. Furthermore, NEPI has prospects in treating hypotension, bronchial asthma and coronary heart diseases [4]. There are several diseases in which NEPI level deviations have been reported to be abnormal: depression, migraine, anxiety, neuroblastoma and paraganglioma [5]. Side effects of NEPI may include vomiting, headache, nausea, dizziness, hypertension and tachycardia, among others. Thus, the precise and sensitive detection of NEPI is of high importance both from a basic physiological research perspective and in a clinical diagnostic setting. Acetaminophen (ACP) or paracetamol is one of the most frequently used analgesics and antipyretics for mild to moderate pain and fever reduction, respectively [6,7]. Since it is efficacious and has few side effects at recommended doses [8,9], it is often used to treat headaches, myalgia, arthritis, and the common cold. Nevertheless, the therapeutic index of AC is narrow, and overdose could result in severe hepatic injury [10], which implies that its precise analytic method is indispensable, particularly when combined with other drugs. The possibility of hepatotoxicity with ACP and its use in therapeutic and non-prescription forms points out the necessity for a reliable and accurate screening test for safe use [11]. It is important to precisely quantify ACP in clinical samples to avoid toxicity and achieve the desired therapeutic effects. ACP is an electroactive compound, and its signal can overlap with that of NEPI, causing a serious interference in the traditional electrochemical detection. Thus, selective and precise detection of NEPI in the presence of ACP is critical for reliable neurochemical analysis and clinical diagnosis. At present, NEPI and ACP are detected by chromatography [12,13], capillary electrophoresis [14,15], chemiluminescence [16], colorimetric method [17,18], fluoro-metric method and spectrophotometry [20,21] in common detection methods; however, certain methods have the shortcomings of long analysis time, expensive instrumentation investment and complicated sample processing process as well as unsuitable for rapid or portable detection, which hinders their over application.

Compared to the method mentioned above, electrochemical determination has been increasingly focused on because it is an excellent analytical approach for detecting electroactive species, offering relatively inexpensive methods that are easy to use, highly sensitive, and quick to respond [22-25]. Moreover, the strong potential of electrochemical techniques for the miniaturization of analytical systems and their capability for in situ and on-site measurements make electrochemical analysis a suitable option for practical and diagnostic applications. In recent years, the development of advanced electrochemical sensors using functional nanomaterials has emerged as a key focus in electroanalysis [26,27]. This approach offers the possibility to significantly enhance the sensitivity, selectivity, and stability of electrodes, enabling the detection of target analytes even in complex matrices. The integration of nanostructured materials, such as metal and metal-oxide nanoparticles, metal-organic frameworks (MOFs), and carbon-based nanomaterials, *etc.*, provides improved electron transfer kinetics and increased active surface area, making these sensors highly suitable for analytical applications, including clinical diagnostics, environmental monitoring, and pharmaceutical analysis [28-30].

MOFs are crystalline porous materials composed of metal ions coordinated with organic ligands, forming highly ordered networks [31]. Their large surface area, tuneable porosity, and chemical functionality make them attractive for applications in gas storage, separation, catalysis, drug delivery, and chemical sensing [32-35]. In electrochemical analysis, MOFs can serve as effective

electrode modifiers, providing a large surface area and facilitating electron transfer. However, the further application of MOFs for the sensitive detection of compounds is significantly limited by their inherent drawbacks: low stability and poor conductivity. Integrating noble metal nanoparticles (NM NPs) with MOFs is an effective strategy to enhance their electrical conductivity and electrocatalytic activity [36,37].

The present work proposes the construction of an electrochemical sensor for the determination of NEPI in the presence of ACP. The amino-functionalized iron-based metal-organic framework NH_2-MIL-101(Fe) MOF/Pd NPs composite was first prepared and characterized for such applications. Subsequently, the synthesized NH_2-MIL-101(Fe) MOF/Pd NPs composite was immobilized on the SPE surface to evaluate its electrochemical sensing performance for NEPI. The NH_2-MIL-101(Fe) MOF/Pd NPs composite demonstrated superior electrocatalytic performance towards NEPI oxidation compared with the bare SPE. The anodic peak current (I_{pa}) demonstrated good linearity with NEPI concentration over the range of 0.02 to 575.0 µM with a detection limit (LOD) of 0.007 µM. Furthermore, the developed sensor enabled simultaneous determination of NEPI and ACP. The sensing platform was successfully used for the determination of NEPI and ACP in real samples, demonstrating its practical applicability.

Materials and methods

Materials

Iron(III) chloride hexahydrate ($FeCl_3 \cdot 6H_2O$), 2-aminoterephthalic acid, N,N-dimethylformamide (DMF), ethanol, palladium chloride ($PdCl_2$), acetonitrile, sodium borohydride ($NaBH_4$), NEPI, ACP, phosphoric acid (H_3PO_4), sodium hydroxide (NaOH) and other chemicals were used in this study. They were obtained from Sigma-Aldrich Company.

Electrochemical experiments

Cyclic voltammetry (CV), differential pulse voltammetry (DPV) and chronoamperometry experiments were used to study the electrochemical sensing platform of the NH_2-MIL-101(Fe) MOF/Pd NPs/SPE for the simultaneous determination of NEPI and ACP. These electrochemical experiments were performed using an electrochemical workstation (CHI660E, CH Instruments, USA) connected to a PC at room temperature (25 ± 1 °C).

Synthesis of NH_2-MIL-101(Fe) MOF/Pd NPs composite

The preparation of NH_2-MIL-101(Fe) MOF/Pd NPs was initiated by the synthesis of NH_2-MIL--101(Fe) MOF, which was carried out as described in previous work using the approach developed by Su *et al.* [38]. Then, 0.05 g of as-synthesized NH_2-MIL-101(Fe) MOF was dispersed in 2 mL of acetonitrile and ultrasonicated for 1 h to form a uniform suspension. $PdCl_2$ (0.05 g) was dissolved in 2 mL of acetonitrile using magnetic stirring at room temperature for 15 min, until the solution turned clear. Subsequently, $PdCl_2$ precursor was dropwise added to the MOF suspension and was continuously stirred with magnetic stirring for another 6 h, then $NaBH_4$ (0.09 g) dissolved in 4 mL ethanol was also dropwise added into this suspension and further stirred for an additional 1 h. The as-obtained precipitate was isolated by centrifugation and washed several times with acetonitrile. The resultant precipitation was further dried under vacuum at 65 °C overnight.

Preparation of NH_2-MIL-101(Fe) MOF/Pd NPs composite-modified SPE

Firstly, 0.25 g of NH_2-MIL-101(Fe) MOF/Pd NPs was suspended in 250.0 µL of distilled water and ultrasonicated for approximately 30 min. Thereafter, 5.0 µL of this suspension was dropped on the surface of the SPEs and left to dry in air.

To estimate the electroactive surface area (A) of bare SPE and NH_2-MIL-101(Fe) MOF/Pd NPs/SPE, CV studies were performed at various scan rates (ν) in a 0.1 M KCl solution containing 5.0 mM $[Fe(CN)_6]^{3-/4-}$. Based on these studies and the Randles-Ševčik equation [39], the values of A were obtained as 0.032 cm^2 for bare SPE and 0.09 cm^2 for NH_2-MIL-101(Fe) MOF/Pd NPs/SPE, respectively.

Results and discussion

NH_2-MIL-101(Fe) MOF/Pd NPs composite characterization

The FE-SEM images of NH_2-MIL-101(Fe) MOF/Pd NPs composite are displayed in Figure 1. The FE-SEM images clearly indicate the presence of NH_2-MIL-101(Fe) MOF and Pd NPs in the prepared composite.

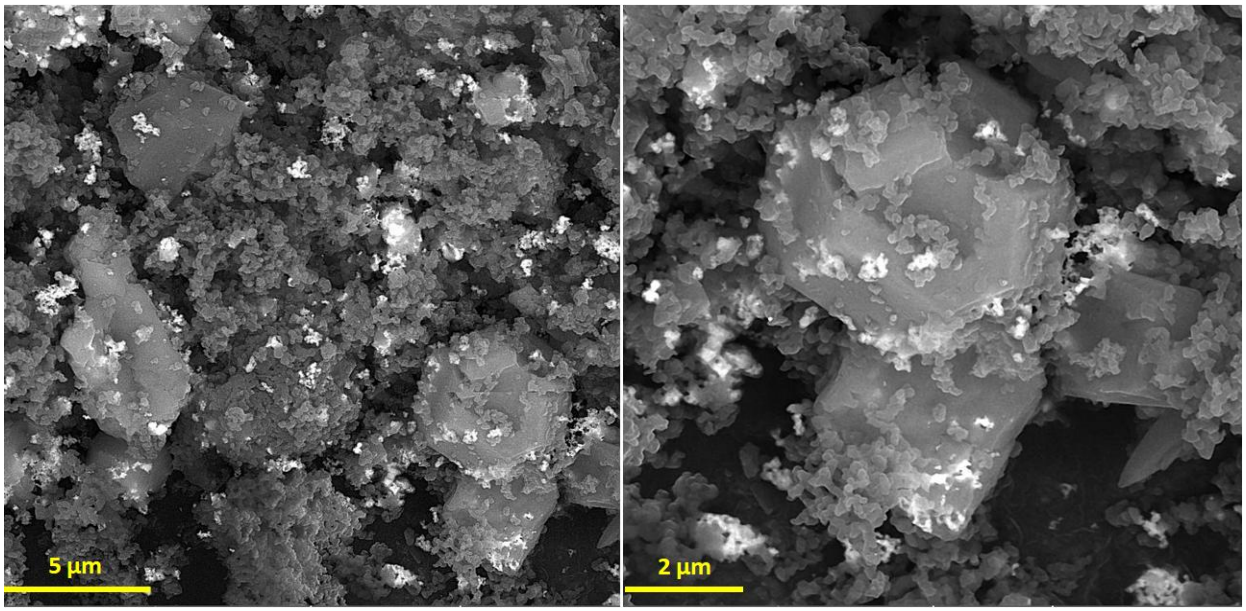

Figure 1. *FE-SEM images of NH_2-MIL-101(Fe) MOF/Pd NPs composite at different magnifications*

Cyclic voltammetry behaviour of NEPI at the bare SPE and the NH_2-MIL-101(Fe) MOF/Pd NPs/SPE

The effect of pH on the voltammetric behaviour of NEPI at the NH_2-MIL-101(Fe) MOF/Pd NPs/SPE was evaluated over pH 4.0-9.0 in 0.1 M phosphate buffer saline (PBS). From the recorded CV responses, the anodic peak current (I_{pa}) of NEPI increases with increasing pH up to 7.0, reaching a maximum at pH 7.0. Further increases in pH do not enhance the peak current; instead, the response gradually decreases. Correspondingly, pH 7.0 was selected as the optimal pH for the subsequent experiments.

Figure 2 shows the CV responses of bare SPE and NH_2-MIL-101(Fe) MOF/Pd NPs-modified SPE in 300.0 µM NEPI solution. The oxidation peak of NEPI appeared at the surface of both SPEs. No cathodic peak is observed in the reverse potential scan, confirming that the electrochemical behaviour of NEPI is completely irreversible. The recorded cyclic voltammograms showed that a low peak current (I_{pa} = 3.0 µA) was observed at the bare SPE, whereas the NH_2-MIL-101(Fe) MOF/Pd NPs-modified SPE demonstrated a well-anodic peak. Furthermore, under the same conditions, NH_2-MIL-101(Fe) MOF/Pd NPs/SPE exhibited a higher anodic peak current (I_{pa}) of about 10.6 µA than that of bare SPE (3.1 µA). Also, the NH_2-MIL-101(Fe) MOF/Pd NPs/SPE showed a lower overpotential

than the bare SPE for the oxidation of NEPI. The synergistic effect between NH_2-MIL-101(Fe) MOF and Pd NPs was mainly responsible for the improved response peak current and decreased over-potential. Particularly, NH_2-MIL-101(Fe) MOF demonstrated higher electrocatalytic activity for the oxidation of NEPI when the electrical conductivity was enhanced by combining with Pd NPs.

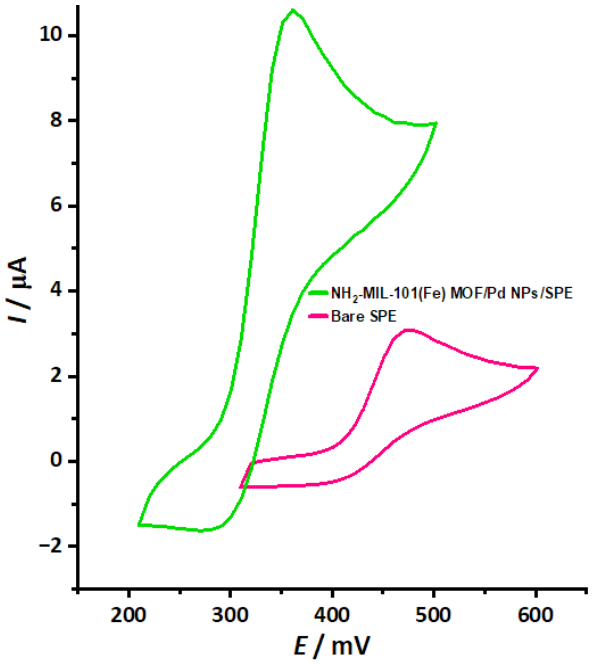

Figure 2. *CV responses of bare SPE and NH_2-MIL-101(Fe) MOF/Pd NPs/SPE in 0.1 mol L-1 PBS (pH 7.0) solution containing 300.0 µM NEPI solution (scan rate: 0.05 V s^{-1})*

Scan rate dependence

To investigate the possible mechanism involved in the electrochemical reaction, the influence of scan rate on the oxidation process of 100.0 µM NEPI solution at the NH_2-MIL-101(Fe) MOF/ /Pd NPs/SPE has been conducted using the CV method for different scan rates. The recorded CVs at different scan rates are exhibited in Figure 3.

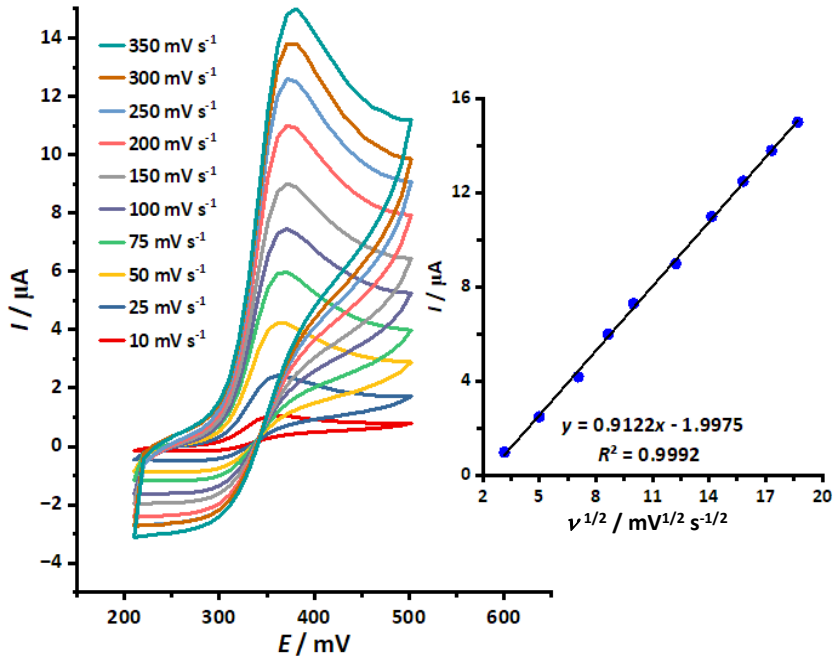

Figure 3. *CVs of NH_2-MIL-101(Fe) MOF/Pd NPs/SPE in 0.1 mol L^{-1} PBS (pH 7.0) solution containing 100.0 µM NEPI at various scan rates. Inset: relationship between I_{pa} and $\nu^{1/2}$*

As shown in the recorded CVs, the oxidation peaks of NEPI shifted to slightly more positive potentials with increasing scan rate, accompanied by concurrent increases in the response peak currents. A linear relationship was obtained between I_{pa} and $\nu^{1/2}$; therefore, the oxidation process of NEPI is diffusion-controlled (Figure 3, Inset).

Chronoamperometric studies of NEPI oxidation at the NH_2-MIL-101(Fe) MOF/Pd NPs/SPE

Because the oxidation reaction was a diffusion-controlled process, the chronoamperometric responses of NH_2-MIL-101(Fe) MOF/Pd NPs/SPE to NEPI solutions with different concentrations were recorded to determine the mean diffusion coefficient (D) of NEPI. The corresponding chronoamperometric responses are displayed in Figure 4. For each chronoamperogram recorded at varying concentrations, the I *vs.* $t^{-1/2}$ curves were plotted, showing a linear correlation in all cases (Figure 4A). The slopes derived from the linear fits were then plotted against the corresponding NEPI concentrations, and the resulting linear curve is presented in Figure 4B. The diffusion coefficient (D) of NEPI was finally calculated to be 1.58×10^{-6} cm^2 s^{-1}, derived from the slope of the linear curve in Figure 4B using the Cottrell equation for a diffusion-controlled mechanism.

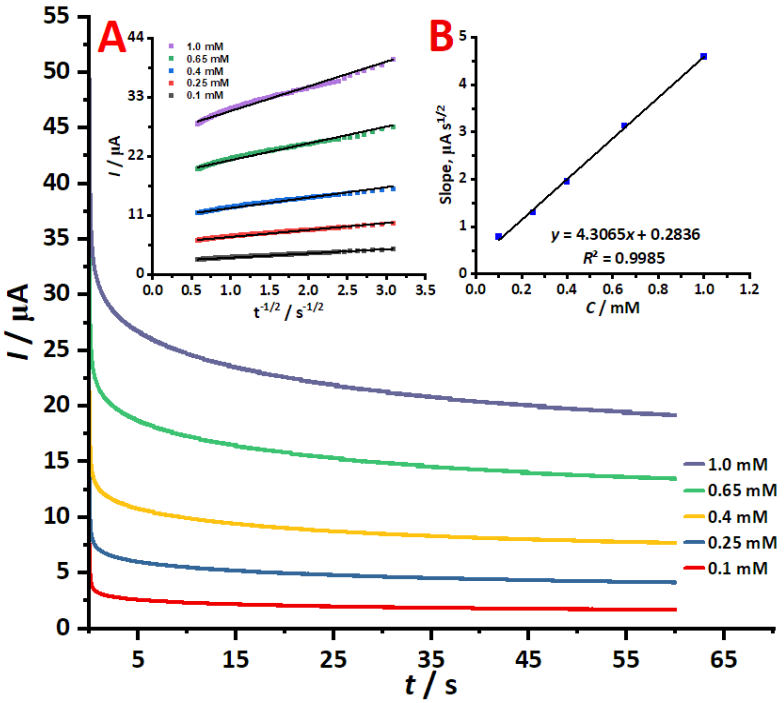

Figure 4. *Chronoamperograms of NH_2-MIL-101(Fe) MOF/Pd NPs/SPE in 0.1 mol L^{-1} PBS (pH 7.0) containing different concentrations of NEPI. Inset A: extracted linear dependence between* I *and* $t^{-1/2}$ *from the obtained chronoamperograms; Inset B: plot of the corresponding slopes versus the concentrations of NEPI*

Quantitative measurements of NEPI using DPV method

DPV was used as a sensitive electrochemical method to quantify NEPI concentrations at the NH_2-MIL-101(Fe) MOF/Pd NPs/SPE, and the resulting voltammograms exhibited well-defined, concentration-dependent oxidation peaks (Figure 5). An enhancement in the peak current of DPV responses was observed as the concentration of NEPI increased. The calibration curve obtained under the optimum conditions demonstrated linearity over a range of 0.02 to 575.0 µM, with the response expressed as shown below: $I = 0.0327C + 1.1088$ ($R^2 = 0.9997$) (Figure 5, Inset). Moreover, the LOD was calculated as 0.007 µM using the following formula: LOD = 3 standard deviations of the blank response divided by the slope of the calibration curve.

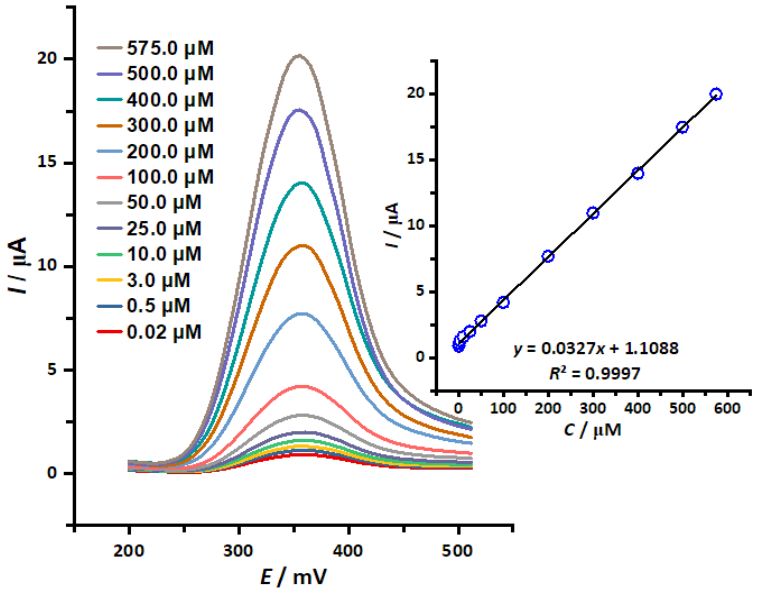

Figure 5. *DPVs of NH_2-MIL-101(Fe) MOF/Pd NPs/SPE in 0.1 mol L^{-1} PBS (pH 7.0) containing different concentrations of NEPI. Inset: calibration plot from the linear relationship between the I_{pa} and concentration of NEPI*

Simultaneous determination of NEPI and ACP at the NH_2-MIL-101(Fe) MOF/Pd NPs/SPE sensing platform

The feasibility of determining NEPI in the presence of ACP at the NH_2-MIL-101(Fe) MOF/Pd NPs/SPE surface was also investigated using DPV. For this purpose, the concentrations of these analytes were varied simultaneously in PBS, and the corresponding DPVs are presented in Figure 6. The DPV responses exhibit two well-separated oxidation peaks for NEPI and ACP at 360 mV and 550 mV, respectively. From the recorded DPV responses, when NEPI and ACP concentrations increase simultaneously, the anodic peak currents increase gradually. Furthermore, the DPV measurements showed a linear increase in peak currents with concentration, ranging from 0.5 to 500.0 µM for NEPI and from 1.0 to 800.0 µM for ACP. The calibration curves of NEPI and ACP are presented in Figure 6.

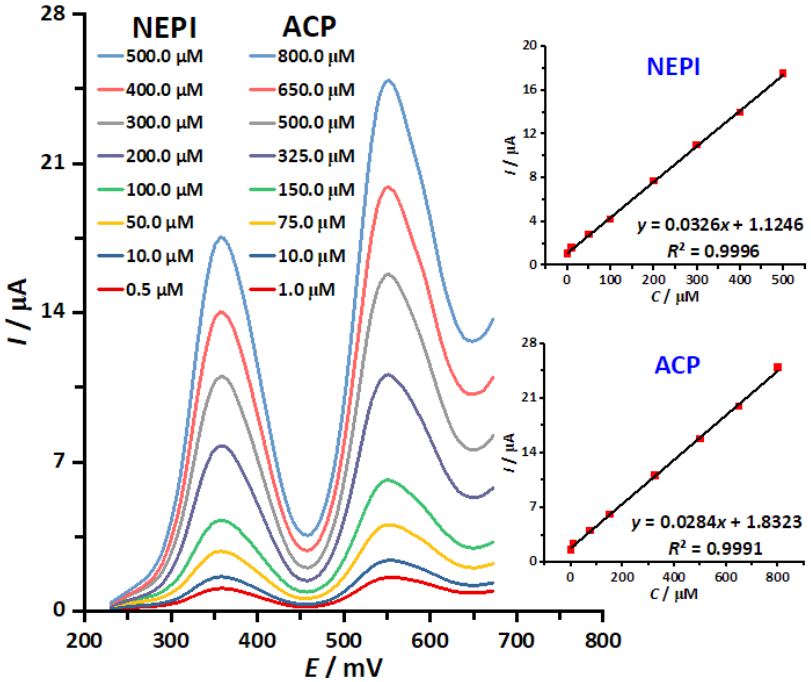

Figure 6. *DPVs of NH_2-MIL-101(Fe) MOF/Pd NPs/SPE in 0.1 mol L-1 PBS (pH 7.0) for simultaneous determination of NEPI and ACP of different concentrations. Insets: corresponding calibration plots for NEPI and ACP*

Determination of NEPI and ACP in various samples

To show the practical application of the designed electrochemical sensor, DPV was performed to determine the concentrations of NEPI and ACP in urine, NEPI ampoule, and ACP tablet samples. The results are summarized in Table 1, which presents the corresponding measured values. Then, these samples were spiked with NEPI solutions at different concentrations. The obtained results exhibited good recovery percentages, from 97.1 to 104.4 %. Moreover, the results demonstrate RSDs ≤ 3.6 % across five measurements. These results show that the designed NH_2-MIL-101(Fe) MOF/Pd NPs/SPE sensor is efficient for the determination of NEPI and ACP and has promise in practical applications.

Table 1. *NEPI and ACP determination and recovery results in urine, NEPI ampoule, and ACP tablet samples using the NH_2-MIL-101(Fe) MOF/Pd NPs/SPE sensing platform*

Sample	Concentration, μM				Recovery, %		RSD, %	
	Spiked		Found					
	NEPI	ACP	NEPI	ACP	NEPI	ACP	NEPI	ACP
Urine	0	0	-	-	-	-	-	-
	5.0	5.5	4.9	5.6	98.0	101.8	3.1	2.3
	7.0	7.5	7.3	7.4	104.3	98.7	2.0	2.8
NEPI ampoule	0	0	2.9	-	-	-	3.3	-
	2.0	4.0	5.0	6.7	102.0	97.1	1.9	2.7
	4.0	6.0	3.9	9.0	97.5	101.1	2.4	3.6
ACP tablet	0	0	-	5.1	-	-	-	2.8
	4.5	1.0	4.7	6.0	104.4	98.4	3.1	1.9
	6.5	3.0	6.4	8.3	98.5	102.5	2.1	3.0

Conclusions

This work indicates the successful application of NH_2-MIL-101(Fe) MOF/Pd NPs composite-modified SPE for sensitive electrochemical determination of NEPI in the presence of ACP. By taking advantage of NH_2-MIL-101(Fe) MOF and Pd NPs, as well as their synergistic effects, the oxidation of NEPI was significantly enhanced. This improvement played a key role in achieving a low LOD of 0.007 μM and a high sensitivity of 0.0327 μA μM^{-1} for NEPI determination. Moreover, the sensor enabled simultaneous determination of NEPI and ACP using the DPV method with high efficiency. The suggested method has been applied for the determination of NEPI and ACP in urine and pharmaceutical formulations. The recoveries obtained were in the range of 97.1 to 104.4 %, which indicates the analytical usefulness of the NH_2-MIL-101(Fe) MOF/Pd NPs composite-modified SPE for the determination of these target compounds in real samples.

Funding: *No funding was received for this study.*

Conflict of interest: *The authors declare that there is no conflict of interest*

References

[1] E. A. Khudaish, A. Al-Badri, A modified Hummers soft oxidative method for functionalization of CNTs: Preparation, characterization and potential application for selective determination of norepinephrine, *Synthetic Metals* **277** (2021) 116803. https://doi.org/10.1016/j.synthmet.2021.116803

[2] M. A. Farahmand Nejad, F. Ghasemi, M. R. Hormozi-Nezhad, A wide-color-varying ratiometric nanoprobe for detection of norepinephrine in urine samples, *Analytica Chimica Acta* **1039** (2018) 124-131. https://doi.org/10.1016/j.aca.2018.07.043

[3] N. Ally, N. Hendricks, B. Gumbi, A colorimetric detection of noradrenaline in wastewater using citrate-capped colloidal gold nanoparticles probe, *Colloids and Interfaces* **6** (2022) 61. https://doi.org/10.3390/colloids6040061

[4] R. N. Goyal, M. A. Aziz, M. Oyama, S. Chatterjee, A. R. S. Rana, Nanogold based electrochemical sensor for determination of norepinephrine in biological fluids, *Sensors and Actuators B* **153** (2011) 232-238. https://doi.org/10.1016/j.snb.2010.10.041
[5] D. Ji, Z. Shi, Z. Liu, S. S. Low, J. Zhu, T. Zhang, Z. Chen, X. Yu, Y. Lu, D. Lu, Q. Liu, Smartphone-based square wave voltammetry system with screen-printed graphene electrodes for norepinephrine detection, *Smart Materials in Medicine* **1** (2020) 1-9. https://doi.org/10.1016/j.smaim.2020.02.001
[6] Y. Dong, M. Zhou, L. Zhang, 3D multiporous Co, N co-doped MoO_2/MoC nanorods hybrids as improved electrode materials for highly sensitive simultaneous determination of acetaminophen and 4-aminophenol, *Electrochimica Acta* **302** (2019) 56-64. https://doi.org/10.1016/j.electacta.2019.02.006
[7] B. R. Adhikari, M. Govindhan, A. Chen, Sensitive detection of acetaminophen with graphene-based electrochemical sensor, *Electrochimica Acta* **162** (2015) 198-204. https://doi.org/10.1016/j.electacta.2014.10.028
[8] N. S. Anuar, W. J. Basirun, M. Ladan, M. Shalauddin, M. S. Mehmood, Fabrication of platinum nitrogen-doped graphene nanocomposite modified electrode for the electrochemical detection of acetaminophen, *Sensors and Actuators B* **266** (2018) 375-383. https://doi.org/10.1016/j.snb.2018.03.138
[9] Y. Zhang, X. Jiang, J. Zhang, H. Zhang, Y. Li, Simultaneous voltammetric determination of acetaminophen and isoniazid using MXene modified screen-printed electrode, *Biosensors and Bioelectronics* **130** (2019) 315-321. https://doi.org/10.1016/j.bios.2019.01.043
[10] K. V. Kavya, D. Muthu, S. Varghese, D. Pattappan, R. R. Kumar, Y. Haldorai, Glassy carbon electrode modified by gold nanofibers decorated iron metal-organic framework nanocomposite for voltammetric determination of acetaminophen, *Carbon Letters* **32** (2022) 1441-1449. https://doi.org/10.1007/s42823-022-00373-3
[11] L. L. Mazaleuskaya, K. Sangkuhl, C. F. Thorn, G. A. FitzGerald, R. B. Altman, T. E. Klein, PharmGKB summary: pathways of acetaminophen metabolism at the therapeutic versus toxic doses, *Pharmacogenetics and Genomics* **25** (2015) 416-426. http://dx.doi.org/10.1097/FPC.0000000000000150
[12] D. G. Ferrer, A. G. García, J. Peris-Vicente, J. V. Gimeno-Adelantado, J. Esteve-Romero, Analysis of epinephrine, norepinephrine, and dopamine in urine samples of hospital patients by micellar liquid chromatography, *Analytical and Bioanalytical Chemistry* **407** (2015) 9009-9018. https://doi.org/10.1007/s00216-015-9066-7
[13] T. Gicquel, J. Aubert, S. Lepage, B. Fromenty, I. Morel, Quantitative analysis of acetaminophen and its primary metabolites in small plasma volumes by liquid chromatography–tandem mass spectrometry, *Journal of Analytical Toxicology* **37** (2013) 110-116. https://doi.org/10.1093/jat/bks139
[14] Y. Hu, X. Wei, Enantioseparation and determination of norepinephrine, epinephrine and isoproterenol by capillary electrophoresis-indirect electrochemiluminescence in human serum, *Current Analytical Chemistry* **14** (2018) 504-511. https://doi.org/10.2174/1573411013666170929150919
[15] A. Ciurba, G. Hancu, L. M. Cojocea, E. Sipos, N. Todoran, Development of new formulation and its evaluation by capillary electrophoresis of tablets containing tramadol hydrochloride and paracetamol, *Pharmaceutical Development and Technology* **19** (2014) 833-838. https://doi.org/10.3109/10837450.2013.836219
[16] Y. J. Chao, L. X. Xie, W. Cao, Chemiluminescence enhancement effect for the determination of acetaminophen with the catalysis of manganese deuteroporphyrin (Mn (III) DP), *Key Engineering Materials* **575** (2014) 249-252. https://doi.org/10.4028/www.scientific.net/KEM.575-576.249
[17] T. M. Godoy-Reyes, A. M. Costero, P. Gavina, R. Martinez-Manez, F. Sancenon, A colorimetric probe for the selective detection of norepinephrine based on a double molecular recognition with functionalized gold nanoparticles, *ACS Applied Nano Materials* **2** (2019) 1367-1373. https://doi.org/10.1021/acsanm.8b02254
[18] F. Shihana, D. Dissanayake, P. Dargan, A. Dawson, A modified low-cost colorimetric method for paracetamol (acetaminophen) measurement in plasma, *Clinical Toxicology* **48** (2010) 42-46. https://doi.org/10.3109/15563650903443137
[19] Y. Zhang, B. Wang, H. Xiong, W. Wen, N. Cheng, A ratiometric fluorometric epinephrine and norepinephrine assay based on carbon dot and CdTe quantum dots nanocomposites, *Microchemical Journal* **146** (2019) 66-72. https://doi.org/10.1016/j.microc.2018.12.060

[20] E. Y. Hashem, A. K. Youssef, Spectrophotometric determination of norepinephrine with sodium iodate and determination of its acidity constants, *Journal of Applied Spectroscopy* **80** (2013) 258-264. https://doi.org/10.1007/s10812-013-9755-y
[21] E. Souri, S. A. M. Nasab, M. Amanlou, M. B. Tehrani, Development and validation of a rapid derivative spectrophotometric method for simultaneous determination of acetaminophen, ibuprofen and caffeine, *Journal of Analytical Chemistry* **70** (2015) 333-338. https://doi.org/10.1134/S1061934815030041
[22] M. Su, X. Cao, H. Gao, C. Zhu, W. Peng, Q. Jiang, C. Yu, Honeycomb-like nickel oxide-reduced graphene oxide based sensor for the electrochemical tracking of norepinephrine in neuronal cells, *Analytica Chimica Acta* **1262** (2023) 341247. https://doi.org/10.1016/j.aca.2023.341247
[23] H. Elshafie, S. B. Changalasetty, A. Mubarakali, Pt-doped reduced graphene oxide-porphyrin-CNT composite-based electrochemical sensor for simultaneous detection of dopamine, serotonin and norepinephrine, *Journal of The Electrochemical Society* **172** (2025) 027507. https://doi.org/10.1149/1945-7111/adb187
[24] A. E. Vilian, S. M. Chen, Y. T. Hung, M. A. Ali, F. M. Al-Hemaid, Electrochemical oxidation and determination of norepinephrine in the presence of acetaminophen using MnO_2 nanoparticle decorated reduced graphene oxide sheets, *Analytical Methods* **6** (2014) 6504-6513. https://doi.org/10.1039/C4AY00878B
[25] V. N. Palakollu, T. E. Chiwunze, C. Liu, R. Karpoormath, Electrochemical sensitive determination of acetaminophen in pharmaceutical formulations at iron oxide/graphene composite modified electrode, *Arabian Journal of Chemistry* **13** (2020) 4350-4357. https://doi.org/10.1016/j.arabjc.2019.08.001
[26] Z. Li, X. Lu, G. Liu, L. Yang, F. Gao, Core-shell ZnO@CoO nitrogen doped nano-composites as highly sensitive electrochemical sensor for organophosphate pesticides detection, *Analytical Biochemistry* **686** (2024) 115422. https://doi.org/10.1016/j.ab.2023.115422
[27] M. Ghalkhani, E. Sohouli, Z. S. Dehkordi, Electrochemical sensor based on mesoporous g-C_3N_4/N-CNO/gold nanoparticles for measuring oxycodone, *Scientific Reports* **14** (2024) 17221. https://doi.org/10.1038/s41598-024-68310-0
[28] Y. Yue, X. Zhang, Z. Xu, L. Sun, S. Li, R. Liu, Ultrasensitive detection of PSA in human serum using Label-Free electrochemical biosensor with magnetically induced Self-Assembly based on α-Fe_2O_3/Fe_3O_4@Au nanocomposites, *Microchemical Journal* **201** (2024) 110487. https://doi.org/10.1016/j.microc.2024.110487
[29] J. D. Priscillal, J. K. Sheu, S. F. Wang, Nanoengineered electrochemical sensor for sensitive detection of carbendazim in environmental waters using Er_3NbO_7/f-CNF nanocomposite, *Environmental Research* **263** (2024) 119927. https://doi.org/10.1016/j.envres.2024.119927
[30] A. Gutiérrez, M. G. Ramírez-Ledesma, G. A. Rivas, G. Luna-Bárcenas, R. A. Escalona-Villalpando, J. Ledesma-García, Development of an electrochemical sensor for the quantification of ascorbic acid and acetaminophen in pharmaceutical samples, *Journal of Pharmaceutical and Biomedical Analysis* **249** (2024) 116334. https://doi.org/10.1016/j.jpba.2024.116334
[31] V. F. Yusuf, N. I. Malek, S. K. Kailasa, Review on metal–organic framework classification, synthetic approaches, and influencing factors: applications in energy, drug delivery, and wastewater treatment, *ACS Omega* **7** (2022) 44507-44531. https://doi.org/10.1021/acsomega.2c05310
[32] R. Ben-Mansour, N. A. Qasem, An efficient temperature swing adsorption (TSA) process for separating CO_2 from CO_2/N_2 mixture using Mg-MOF-74, *Energy Conversion and Management* **156** (2018) 10-24. https://doi.org/10.1016/j.enconman.2017.11.010
[33] S. Govindaraju, S. K. Arumugasamy, G. Chellasamy, K. Yun, Zn-MOF decorated bio activated carbon for photocatalytic degradation, oxygen evolution and reduction catalysis, *Journal of Hazardous Materials* **421** (2022) 126720. https://doi.org/10.1016/j.jhazmat.2021.126720
[34] M. P. Abuçafy, A. S. Mori, B. L. Caetano, S. J. L. Ribeiro, L. A. Chiavacci, Cyclodextrin-metal-organic framework (CD-MOF)/organic-inorganic hybrid composite as a potential material for drug delivery devices, *Journal of Molecular Structure* **1314** (2024) 138717. https://doi.org/10.1016/j.molstruc.2024.138717
[35] T. Wiwasuku, J. Boonmak, K. Siriwong, V. Ervithayasuporn, S. Youngme, Highly sensitive and selective fluorescent sensor based on a multi-responsive ultrastable amino-functionalized Zn (II)-MOF for

hazardous chemicals, *Sensors and Actuators B* **284** (2019) 403-413. https://doi.org/10.1016/j.snb.2018.12.094

[36] S. Wang, D. Wang, M. Li, S. Wang, S. Xiang, K. Feng, Q. Liu, P. Wang, Y. Li, F. Tang, Interfacial galvanic replacement strategy for Pd-doped NiFe MOF nanosheets with highly efficient dopamine detection, *Microchimica Acta* **191** (2024) 280. https://doi.org/10.1007/s00604-024-06359-4

[37] A. T. Ezhil Vilian, B. Dinesh, R. Muruganantham, S. R. Choe, S. M. Kang, Y. S. Huh, Y. K. Han, A screen printed carbon electrode modified with an amino-functionalized metal organic framework of type MIL-101 (Cr) and with palladium nanoparticles for voltammetric sensing of nitrite, *Microchimica Acta* **184** (2017) 4793-4801. https://doi.org/10.1007/s00604-017-2513-8

[38] S. Su, Z. Xing, S. Zhang, M. Du, Y. Wang, Z. Li, W. Zhou, Ultrathin mesoporous g-C_3N_4/NH_2-MIL-101 (Fe) octahedron heterojunctions as efficient photo-Fenton-like system for enhanced photo-thermal effect and promoted visible-light-driven photocatalytic performance, *Applied Surface Science* **537** (2021) 147890. https://doi.org/10.1016/j.apsusc.2020.147890

[39] R. S. Santos, L. F. Felipe, G. N. Meloni, Theory in Practice: Testing the Limits of the Randles–Ševčík Equation. ACS Electrochemistry **2** (2026) 478-485. https://doi.org/10.1021/acselectrochem.5c00457